“Full Fusion” is not Ineluctable during Vesicular Exocytosis of Neurotransmitters by Endocrine Cells

Alexander Oleinick, Irina Svir, Christian Amatore*

Ecole Normale Supérieure-PSL Research University, Département de Chimie, Sorbonne Universités-UPMC Univ. Paris 06, CNRS UMR 8640 PASTEUR, 24 rue Lhomond, 75005 Paris, France.

Abstract:

Vesicular exocytosis is an essential and ubiquitous process in neurons and endocrine cells by which neurotransmitters are released in synaptic clefts or extracellular fluids. It involves the fusion of a vesicle loaded with chemical messengers with the cell membrane through a nanometric fusion pore. In endocrine cells, unless it closes after some flickering (“Kiss-and-Run” events), this initial pore is *supposed* to expand exponentially leading to a full integration of the vesicle membrane into the cell one, a stage called “full fusion”. We report hereafter a compact analytical formulation that allows extracting precise measurements of the fusion pore expansion extent and rate from individual amperometric spikes time-courses. These data definitively establish that during release of catecholamines fusion pores enlarge at most to ca. one fifth of the radius of their parent vesicle, hence ruling out the ineluctability of “full fusion”.

Keywords: exocytosis • vesicle • full fusion • endocrine cell • fusion pore

* Corresponding author: christian.amatore@ens.fr

Introduction

The high importance of vesicular exocytosis in biology and medicine is evidenced, among many other examples [1-6], by two recent Nobel prizes of physiology and medicine, the latest one being awarded in 2013 to James E. Rothman, Randy W. Schekman, and Thomas C. Südhof [3-6]. In neurons and endocrine cells neurotransmitters are transported as cargoes by vesicles tailored and loaded in the Golgi apparatuses to be finally delivered at specific release sites of the cell membrane where they dock to finally release neurotransmitters through a fusion pore connecting the cell and vesicle membranes [7-12]. In endocrine cells, release through the initial fusion pore is minute and the pore may close or flicker (Kiss-and-Run) [13-21] as occurs in neurons [22-24] but generally rapidly expands [25] to release a massive flux of neurotransmitter that is precisely quantifiable by amperometry at carbon fibres micro- and nanoelectrodes [22-24, 26-34]. This stage is generally considered to end in a full integration of the vesicle membrane into the cell one, hence its “full fusion” designation. There is a wealth of data characterizing in deep details vesicles formation, transport and SNAREs-assisted docking stages as well as the initial fusion pore size and flickering dynamics. However, the ineluctability of the “full fusion” stage has recently become a matter of debate [30-33], though, at least in endocrine cells, it conditions the ultimate purpose of the whole process leading to neurotransmitters release.

Would the fusion pore dynamics be exclusively governed by bilipid membranes energetics [34-36], its enlargement should be driven by the viscous dissipation of tension energies imposed by the important curvatures created at the small fusion pores edges and by the vesicle membrane surface tension [32, 34-36]. The replacement of catecholamine cations by hydrated monovalent ones inside the matrix during release should lead to its swelling [37-40]. However, swelling is necessarily refrained by the presence of the vesicle membrane, at least while the pore radius remains small vs. that of the vesicle [32]. The ensuing internal swelling pressure that builds up in the constrained matrix during release provokes a constant increase of the membrane surface tension and sustains the continuous enlargement of the fusion pore [35, 36]. So in the absence of external factors “full fusion” appears ineluctable. This explains why the occurrence of this stage has become a paradigm in the field. In addition, several TIRFM [25] and EM [15, 41-43] data

support its existence through the report of fusion pores with sizes comparable to those of vesicles.

However, it is not clear whether or not these data represent normal or exceptional events possibly related to another vesicle function [44, 45-48]. Actually, in endocrine cells, depending on the level of excitation and the size of the fusion pore [45-48], exocytotic vesicles ensure a second important function besides the release of small neurotransmitters molecules that is considered here. This second role serves to regulate hormone peptides through release of the chromogranins forming the matrix structure [49-52] followed by their enzymatic digestion. Release of such long highly folded peptidic strands requires that the matrix is swollen and almost fully exposed to the extracellular fluid. This implies the formation of fusion pore with size comparable to that of the former vesicle [45-48] as described by the "full fusion" paradigm and observed by TIRFM and EM. This duality of function is fully coherent with the significant delays observed between fusion pore opening and peptide release by neuroendocrine cells dense-core vesicles [45-48, 52]. Conversely, neurotransmitters are sufficiently small for diffusing within still compact matrixes and high fluxes be released through much smaller fusion pores.

Amperometry at carbon fibres micro- and nanoelectrodes ("artificial synapse") [26, 27] allows recording of statistically relevant series of kinetic measurements of neurotransmitters fluxes emitted by endocrine cells [26-33] or in neuronal synapses [22-24] as soon as the initial fusion pore opens. Albeit the considerable wealth of information provided by amperometry [27, 30], relating fluxes to fusion pores sizes has been unmanageable up to recently. Doing so requires knowing the transport rate of neurotransmitters within vesicle matrixes, $\kappa = D_{\mathrm{ves}}/R_{\mathrm{ves}}^2$, where D_{ves} is the apparent diffusion coefficient [53, 54-63] of the neurotransmitter inside the vesicle matrix of radius R_{ves} [64-66]. Yet, $\kappa = 415\ \mathrm{s}^{-1}$ was determined recently for chromaffin cells [66] based on correlations between current pre-spike-features intensities and initial fusion pore size, $R_{\mathrm{pore}}^{\mathrm{initial}}$, values reported by patch-clamp [20]. This allowed extracting quantitatively the time-course and final values of fusion pores expansion from individual amperometric spikes currents based on heavy and delicate auto-adaptive simulations [23, 24, 64-66]. Though difficultly manageable by non-experts due to the need of human decision at several critical stages [23, 24, 65, 66] such simulations established quantitatively for the first time that most amperometrically-

detected events involve fusion pores whose expansion was stalled at a maximum size of only ca. one tenth that of the vesicle. These results, as well as other evidences inferred by others based on purely experimental strategies [30, 31, 67-70], have instilled the concept that in endocrine cells most releasing events entirely proceed through fusion pores whose radii remain much smaller than those of vesicles, i.e., contradict the "full fusion" paradigm.

These previous simulations provided important knowledge about the dynamics of diffusion within endocrine matrixes during catecholamine release (see a summary of the main points and conclusions in Sections SM1 and SM2 of Supplementary Material (SM)). One key conclusion is that most of the release is governed by a quasi-steady state diffusional regime that is achieved within the vesicle since the very beginning of release. This conclusion leads now to a fast, simple and expedient analytical approach for extracting the time variations of the fusion pore radius, $R_{\mathrm{pore}}(t)$, that we wish to disclose here. This method allows gathering statistically significant sets of data from control cells or from cells submitted to different strains that will then be used to examine whether or not the fusion pore expansion is solely regulated by the energetics and dissipative properties of the cell-vesicle membrane assembly. For this purpose we will take advantage of several sets of amperometric spikes that were published previously by our group [71, 72] and whose classical amperometric characteristics are summarized in Section SM3 of SM.

Results and Discussion

It is now well established that almost all amperometric spikes involve exponentially decaying branches [64-66, 73, 74]. The origin of such behaviour is a direct consequence of the quasi-steady state diffusional regime established within the vesicle (see SM2) when the fusion pore has reached its maximal opening size (see below). In this work we need to restrict to the commonly considered situation in which the current decays following a single-exponential mode though it is noted that a non-negligible fraction of events involve decay branches exhibiting two-exponentials modes [30, 32, 33, 67, 70]. Though the origin of this second class of spikes has been fully rationalized [32], the method developed hereafter cannot be directly applied to such events.

Our previous works [64-66] whose main conclusions are summarized in SM1 and SM2 established that that soon as $\kappa t > 0.1$ (viz., $t > 0.1 \times R_{\mathrm{ves}}^2/D_{\mathrm{ves}} \approx 0.2$ ms for $\kappa = 415\ \mathrm{s}^{-1}$ [66]), i.e., under

all experimental circumstances of interest here, the diffusionally-controlled neurotransmitter concentration pattern established within a releasing vesicle reaches a quasi-steady state regime. Under this regime, at any time the concentration at any point within the matrix is proportional to the time-dependent neurotransmitter average value within the whole matrix, with a scaling factor that depends on the location within the matrix but is independent of time (see Figure SM-1). Note that this property of diffusional leakage from a closed reservoir is universal and is the justification of Newton and Kelvin exponential laws of cooling of solid bodies. It then follows that at any time, t, the flux of catecholamine cations through the fusion pore (i.e., the concentration gradient at the entrance of the pore) is proportional to the average quantity, $q_{\mathrm{ves}}(t)$, of releasable catecholamines still present inside the vesicle matrix at the same time t. Hence, assuming that the released fluxes are exclusively governed by the convergent diffusion of neurotransmitters inside the matrix towards the entrance of the fusion pore (see SM1 for justification of this model based on our previous works [32, 33, 64-66]), allows to express the time-dependent quantity of releasable catecholamines inside the matrix as:

$$\mathrm{d}q_{\mathrm{ves}}/\mathrm{d}t \ = -\kappa\rho \times q_{\mathrm{ves}}(t) \tag{1}$$

where ρ is a time-dependent coefficient that depends on the value of $R_{\mathrm{pore}}(t)/R_{\mathrm{ves}}$. This justifies the observation of amperometric spikes with single exponential decay current branches. Indeed, as soon as the fusion has reached its time-independent final size $R_{\mathrm{pore}}^{\mathrm{max}}$, the product $\kappa\rho$ becomes a constant. Accordingly, q_{ves} decreases exponentially giving an indirect proof of the quasi-steady state diffusional regime. On the other hand, owing to Faraday's law, the amperometric current is given by:

$$i(t) = -2F(\mathrm{d}q_{ves}/\mathrm{d}t) \tag{2}$$

since the oxidation of any catecholamine molecule at the electrode surface consumes 2 electrons [27]. Hence, the amperometric spikes currents also decay exponentially.

Interestingly, $\rho \cong R_{\mathrm{pore}}(t)/R_{\mathrm{ves}}$ provided that $R_{\mathrm{pore}}(t)/R_{\mathrm{ves}} < 0.7$ [32, 33, 64-66], a condition that applies to all amperometric events treated hereafter (see below), so that Eqn (1) writes as:

$$\mathrm{d}q_{\mathrm{ves}}/q_{\mathrm{ves}} \ = -\kappa[R_{\mathrm{pore}}(t)/R_{\mathrm{ves}}]\mathrm{d}t \tag{3}$$

Noting $q_{\mathrm{ves}}^{\mathrm{tot}}$ the total amount of releasable catecholamine cations in the vesicles, viz.:

$$q_{\mathrm{ves}}^{\mathrm{tot}} = 2F\int_0^{\infty} i(t)dt \tag{4}$$

as follows from Eqn (2), Eqn (1) can be rewritten as:

$$R_{\mathrm{pore}}(t)/R_{\mathrm{ves}} = [i(t)/\kappa]/[2Fq_{\mathrm{ves}}^{\mathrm{tot}} - \int_0^t i(u)\mathrm{d}u] \tag{5}$$

i.e.:

$$R_{\mathrm{pore}}(t) = (R_{\mathrm{ves}}/\kappa) \times [i(t)/\int_t^{\infty} i(u)\mathrm{d}u] \tag{6}$$

(note that in Eqns (5,6) the variable u represent a dummy integration variable related to the time).

By definition, Eqn (6) applies as soon as $t > 0.1/\kappa$, i.e., as soon as the quasi-steady state regime is achieved within the vesicle under scrutiny. Its validity was tested by comparison to the results of our previous rigorous auto-adaptive numerical procedures [23, 24, 64-66] and found accurate within one percent at worst. For and $\kappa = 415\ \mathrm{s}^{-1}$ as determined previously [66, 79], Eqn (6) applies at times larger than ca. 0.2 ms after the beginning of release, viz., virtually describes the whole spikes and their possible pre-spike features (PSF) that correspond to the opening of the initial fusion pore and are observed in ca. 30% of the events [27, 30]. In other words, Eqn (6) describes the full course of release at the exception of the rising part of PSF that describes, when observable, the opening of the initial fusion pore. Indeed, then the release kinetics are certainly governed in part by the transport through the sub-nanometric channel and not only by the convergent diffusion inside the matrix. Indeed, the only hypothesis made in deriving Eqn (6) amounts to assume that the rate of transit across the fusion pore channel is not rate limiting, i.e., that the released flux only depends on the concentration gradients inside the vesicle at the entrance of the fusion pore [65, 66, 75-77]. As recalled in SM1, this is valid as soon as the initial fusion pore has achieved its nanometric initial radius [20] but is probably not before this is achieved.

Finally, it is remarked that an independent knowledge of R_{ves}/κ value is not required for applying Eqn (6) to a series of related individual current spikes that involve releasing events from essentially similar vesicles, viz., belonging to a given cell type. Indeed, would this factor be unknown, $R_{\mathrm{pore}}(t)$ would be obtained on a same relative scale. In the following, $R_{\mathrm{pore}}(t)$ variations are reported on an absolute scale through relying onto the mean $R_{\mathrm{ves}} = 156$ nm vesicle radius reported for chromaffin cells [78] and $\kappa = 415\ \mathrm{s}^{-1}$ as determined previously [66, 79].

Indeed, the size of the initial fusion pore that led to the measurement of $\kappa = 415\ \mathrm{s}^{-1}$ for chromaffin cells is imposed by the architecture of the SNAREs assembly. Hence, this can be considered as invariant even when the membrane is affected by brief external changes in experimental conditions (e.g., osmolality or exogenous lipids trans-insertion; see below).

Two quantitative features are useful for characterizing these curves. One is the maximal size, $R_{\mathrm{pore}}^{\mathrm{max}}$, of the fusion pore (Figures 1A,B) and the other its radial expansion rate, $v_{\mathrm{open}} = \mathrm{d}R_{\mathrm{pore}}(t)/\mathrm{d}t$, represented by its maximum value, $v_{\mathrm{open}}^{\mathrm{max}}$, in Figure 1C. Within the "full fusion" paradigm one would expect that $R_{\mathrm{pore}}^{\mathrm{max}}/R_{\mathrm{ves}} \to 1$ while a significant amperometric current is still monitored. Figures 1A,B establish that this is far from being the case: under all circumstances examined here, $R_{\mathrm{pore}}^{\mathrm{max}}$ median values are ca. one tenth of the mean vesicle radius and remains always lesser than ca. one fifth of it. This same upper limit was observed for controls (Figure 1Ba) or for cells submitted to brief hyper- (Figure 1Bb) or hypotonic (Figure 1Bc) shocks [71] albeit the membrane surface tension was drastically reduced in the first case and drastically increased in the second one compared to controls (compare Figures SM-2a-c in SM). These perturbations affect the shapes of $R_{\mathrm{pore}}^{\mathrm{max}}$ distributions in Figure 1B (see Table 1 for median and quartile values), increasing the probability of small $R_{\mathrm{pore}}^{\mathrm{max}}$ values under hypertonic conditions (Figure 1Bb, lowly tensed membranes) and of large ones for hypotonic ones (Figure 1Bc, highly tensed membranes). Within a mechanical perspective, both changes are coherent with the expected decrease or increase, respectively, of surface tensions, i.e., of the driving force powering the fusion pore expansion [34-36, 75-77]. Nonetheless, one observes that $R_{\mathrm{pore}}^{\mathrm{max}} < 30\ \mathrm{nm}$ in all cases (normal, hyper- or hypotonic conditions) suggesting that this limit does not depend on the membrane characteristics though, as expected, it is more frequently reached for tense membranes than for relaxed ones.

Another set of experiments involved cells submitted to brief micromolar incubations with exogenous bilipids with cone angles θ different from that, θ ≈ 0, of the "*cylindrical*" endogenous cell ones, viz., arachidonic acid ("*cone-shaped*", $\theta_{AA} > 0$; Figure 1Bd) or lyso-phosphatidylcholine ("*inverted cone shaped*", $\theta_{LPC} < 0$; Figure 1Be) immediately before stimulating release [72], with the perspective of altering the fusogenic and dissipative properties of the membrane assembly [80-85]. The brief incubations ensured that exogenous lipids exclusively *trans*-inserted in the

outer leaflet of the cell membrane [84] with opposite consequences on the large positive curvatures at the fusion pores edges [36, 64-66, 75-77, 86, 87] due to their shapes. Figure 1Bd confirms the unfavourable effect of the negative curvatures promoted by AA [86, 87]. Contrariwise, as expected, LPC favours positive curvatures [84, 85] and shifts $R_{\mathrm{pore}}^{\mathrm{max}}$ distributions towards larger values (Figure 1Be and Table 1). Nonetheless, in both cases, the previous limit at ca. 30 nm holds. This ubiquitous limit strongly suggests that while it expands, the fusion pore tube external wall encounters a biological barrier that blocks its further enlargement beyond this range [88, 89]. Considering that in this work we access to the inner radius of the fusion pore and taking into account that the thickness of a lipidic bilayer ranges between 3 and 4 nm and neglecting the possible presence of membrane proteins in the fusion tube, a probable diameter of the free space in which the fusion pore may expand is ca. 50-70 nm under control conditions. This is a large size but remains still between ca. one sixth to one fourth of a mean vesicle diameter (312 nm [78]). Still, it is noted that such a value is not incompatible with the mesh sizes of sub-membrane cytoskeleton proteic structures [90-93].

Before the fusion pore external edge meets this limit, its radial expansion rate results from a balance between the driving force acting on the pore edge and the ability of the system to relax its released energy through viscous dissipation [35, 36, 75, 76]. Accordingly, $R_{\mathrm{pore}}(t)$ enlarges exponentially at the beginning of its expansion (i.e., before the markers in Figure 1A) [35, 36, 75, 76, 90-93]. After this phase, the rate of expansion progressively levels off while the fusion pore radius reaches its maximum value, $R_{\mathrm{pore}}^{\mathrm{max}}$. $v_{\mathrm{open}}^{\mathrm{max}}$ (Figure 1C) provides a good indication of the expansion velocity before the fusion pore edge may start to significantly interact with the non-lipidic biological structure(s) that ultimately limit(s) its expansion [94].

All $v_{\mathrm{open}}^{\mathrm{max}}$ distributions display exponential tails at large values as is expected for individual rates of single events controlled by a single elementary process [95, 96]. For hypertonic and AA-modified conditions this applies over the whole range of $v_{\mathrm{open}}^{\mathrm{max}}$ values (Figures 1Cb and 1Cd). Conversely, for controls, hypotonic and LPC-modified conditions (respectively in Figures 1Ca,c,e) probability densities in the low $v_{\mathrm{open}}^{\mathrm{max}}$ range result considerably smaller than expected through extrapolating back the upper-range exponential comportment. This phenomenon is exacerbated for hypotonic and LPC-modified conditions compared to controls. We have not yet definite

explanation for the occurrence of such behaviour, but this and the relative effects of hypotonic and LPC-modified conditions vs. controls suggest that at least two factors control the initial fusion pore expansion rate [96]. One possible rationale amounts to consider that the decrease in leaflet-leaflet viscosity [35] due to a high initial surface tension at the end of the SNAREs-constricted phase (controls and hypotonic conditions, Figures 1Ca,c) or to a stabilization of positive curvatures (LPC-modified conditions, Figure 1Ce) facilitates the viscous dissipation of the energy accumulated in the matrix before the fusion pore could expand, hence decreases the observation of low $v_{\mathrm{open}}^{\mathrm{max}}$ values. Still, whatever the exact mechanism(s) underlying such peculiar $v_{\mathrm{open}}^{\mathrm{max}}$ distributions, the data in Figure 1C establish that in all cases the rate of the fusion pore expansion during the first part of its total span strongly depends on the bilipidic membrane properties, confirming what was inferred from $R_{\mathrm{pore}}^{\mathrm{max}}$ distributions (Figure 1B and Table 1). However, this never leads to "full fusion" as would happen if the expansion was controlled only by the membrane properties. Indeed, the fast initial enlargement of the fusion pore is rapidly counteracted by other forces that eventually limit its final radius at ca. 30 nm.

These two series of paired experiments confirm that the membrane tensions forces act in powering the fusion pore enlargement [34-36, 75-77] after its initial SNAREs-stabilized architecture breakdowns [13]. However, the internal pressure within the matrix necessarily continues to build [37-40] during the whole release, thus contributing to increase the surface tension forces even after the fusion pore has reached its maximum value. Nonetheless, these forces result ultimately insufficient to overcome the other ones imposed by the biological barrier(s) [88, 89]. This conclusion is perfectly coherent with recent reports from Ewing et al. who showed that interfering with proteins that are generally considered to be involved in vesicle budding (viz., actin regulating proteins or other cytoplasmic ones such as dynamin) modifies the intensity and time duration of amperometric spikes [69, 70]. In some regards, this is also coherent with the possible interplay between dynamin and myosin described by Smith et al. [45-48] to account for the dichotomy between catecholamines and peptides release by endocrine cells. Though recent reviews still presented such possibilities as "hypothetical" [88, 89], the measurements reported in Figures 1A and 1B provide for the first time a strong quantitative ground to these previous views.

Conclusion

Altogether, the present data provide a first quantitative support to a new paradigm and reject the ineluctability of a "full fusion" outcome when the fusion pore enlarges beyond it SNAREs-stabilized architecture. If the rapid fusion pore expansion is unquestionably promoted by the viscous dissipation of edge and surface tensions energies of vesicle-cell membrane assembly, the corresponding driving forces are rapidly counteracted by other forces that apply as soon as the fusion pore reaches ca. 15-30 nm [30, 67-70]. Within this perspective, the occurrence of the much wider fusion pores observed by TIRFM or EM, a fact that usually substantiates the "full fusion" paradigm, may either be featuring incidental rare events or exocytotic vesicle functions that are not related to neurotransmitter release but possibly to another role such as hormonal peptide regulation [45-52].

Data accessibility

The experimental data used in this work were previously published [71, 72].

Competing interests

The authors declare no competing interest.

Authors' contributions

C.A. designed research; I.S. and A.O. performed research; A.O. wrote computer codes; C.A. prepared the manuscript.

Acknowledgements and Funding

This work was supported in parts by Ecole Normale Supérieure, CNRS, and the University Pierre and Marie Curie (UMR 8640) within the framework of PSL. CA thanks his colleagues and former Ph.D. students who recorded the amperometric spikes analysed in this work based on Eqn (1) and whose classical analyses have been already published in references [71, 72].

Ethics statement

This work was of theoretical nature and, as such, did not involve any ethics infringement.

References and Notes

[1] Stevens CF. 2003 Neurotransmitter Release at Central Synapses. *Neuron* **40**, 381–388. (doi: 10.1016/s0896-6273(03)00643-3)

[2] Gundelfinger ED, Kessels MM, Qualmann B. 2003 Temporal and spatial coordination of exocytosis and endocytosis. *Nat. Rev. Mol. Cell Bio.* **4**, 127–139. (doi: 10.1038/nrm1016)

[3] Sudhof TC, Rizo J. 2011 Synaptic Vesicle Exocytosis. *Cold Spring Harb. Perspect. Biol.* **3**, a005637–a005637. (doi: 10.1101/cshperspect.a005637)

[4] Kaiser CA, Schekman R. 1990 Distinct sets of SEC genes govern transport vesicle formation and fusion early in the secretory pathway. *Cell* **61**, 723–733. (doi: 10.1016/0092-8674(90)90483-u)

[5] McNew JA, Parlati F, Fukuda R, Johnston RJ, Paz K, Paumet F, Sollner TH, Rothman JE. 2000 Compartmental specificity of cellular membrane fusion encoded in SNARE proteins. *Nature* **407**, 153-159. (doi: 10.1038/35025000)

[6] Fernandez-Chacon R, Konigstorfer A, Gerber SH, Garcia J, Matos MF, Stevens CF, Brose N, Rizo J, Rosenmund C, Südhof TC. 2001 Synaptotagmin I functions as a calcium regulator of release probability. *Nature* **410**, 41-49. (doi: 10.1038/35065004)

[7] Langley K, Grant NJ. 1997 Are exocytosis mechanisms neurotransmitter specific? *Neurochem. Int.* **31**, 739–757. (doi: 10.1016/s0197-0186(97)00040-5)

[8] Rituper B, Flašker A, Guček A, Chowdhury HH, Zorec R. 2012 Cholesterol and regulated exocytosis: A requirement for unitary exocytotic events. *Cell Calcium* **52**, 250–258. (doi: 10.1016/j.ceca.2012.05.009)

[9] Jahn R, Fasshauer D. 2012 Molecular machines governing exocytosis of synaptic vesicles. *Nature* **490**, 201-207. (doi: 10.1038/nature11320)

[10] Mohrmann R, de Wit H, Verhage M, Neher E, Sørensen JB. 2010 Fast vesicle fusion in living cells requires at least three SNARE Complexes. *Science* **330**, 502–505. (doi: 10.1126/science.1193134)

[11] Steyer JA, Horstmann H, Almers W. 1997 Transport, docking and exocytosis of single secretory granules in live chromaffin cells. *Nature* **388**, 474-478. (doi: N/A)

[12] Wu LG, Hamid E, Shin W, Chiang HC. 2014 Exocytosis and endocytosis: modes, functions, and coupling mechanisms. *Annu. Rev. Physiol.* **76**, 301–331. (doi: 10.1146/annurev-physiol-021113-170305)

[13] Alabi AA, Tsien RW. 2013 Perspectives on kiss-and-run: role in exocytosis, endocytosis, and neurotransmission. *Annu. Rev. Physiol.* **75**, 393-422. (doi: 10.1146/annurev-physiol-020911-153305)

[14] Rizzoli SO, Jahn R. 2007 Kiss-and-run, collapse and 'readily retrievable' vesicles. *Traffic* **8**, 1137-1144. (doi: 10.1111/j.1600-0854.2007.00614.x)

[15] Fesce R, Grohovaz F, Valtorta F, Meldolesi J. 1994 Neurotransmitter release: fusion or 'kiss-and-run'? *Trends Cell Biol.* **4**, 1-4. (doi: N/A)

[16] Penner R, Neher E. 1988 Secretory responses of rat peritoneal mast cells to high intracellular calcium. *FEBS Letters* **226**, 307–313. (doi: 10.1016/0014-5793(88)81445-5)

[17] Neher E. 1993 Secretion without full fusion. *Nature* **363**, 497–498. (doi: 10.1038/363497a0)

[18] Breckenridge LJ, Almers W. 1987 Currents through the fusion pore that forms during exocytosis of a secretory vesicle. *Nature* **328**, 814–817. (doi: 10.1038/328814a0)

[19] Spruce AE, Breckenridge LJ, Lee AK, Almers W. 1990 Properties of the fusion pore that forms during exocytosis of a mast cell secretory vesicle. *Neuron* **4**, 643–654. (doi: 10.1016/0896-6273(90)90192-i)

[20] Albillos A, Dernick G, Horstmann H, Almers W, de Toledo GA, Lindau M. 1997 The exocytotic event in chromaffin cells revealed by patch amperometry. *Nature* **389**, 509-512. (doi: 10.1038/39081)

[21] Lindau M, Alvarez de Toledo G. 2003 The fusion pore. *Biochim. Biophys. Acta - Mol. Cell Res.* **1641**, 167–173. (doi: 10.1016/s0167-4889(03)00085-5)

[22] Li YT, Zhang SH, Wang L, Xiao RR, Liu W, Zhang XW, Zhou Z, Amatore C, Huang WH. 2014 Nanoelectrode for amperometric monitoring of individual vesicular exocytosis inside single synapses. *Angew. Chem. Int. Ed.* **53**, 12456-12460. (doi: 10.1002/anie.201404744)

[23] Li YT, Zhang SH, Wang XY, Zhang XW, Oleinick AI, Svir I, Amatore C, Huang WH. 2015 Real-time monitoring of discrete synaptic release events and excitatory potentials within self-reconstructed neuromuscular junctions. *Angew. Chem. Int. Ed.* **54**, 9313–9318. (doi: 10.1002/anie.201503801)

[24] Majdi S, Berglund EC, Dunevall J, Oleinick AI, Amatore C, Krantz DE, Ewing AG. 2015 Electrochemical measurements of optogenetically stimulated quantal amine release from single nerve cell varicosities in drosophila larvae. *Angew. Chem. Int. Ed.* **54***,* 13609-13612. (doi: 10.1002/anie.201506743)

[25] Zenisek D, Steyer JA, Almers W. 2000 Transport, capture and exocytosis of single synaptic vesicles at active zones. *Nature* **406**, 849-854. (doi: 10.1038/35022500)

[26] Wightman RM, Jankowski JA, Kennedy RT, Kawagoe KT, Schroeder TJ, Leszczyszyn DJ, Near JA, Diliberto EJ, Viveros OH. 1991 Temporally resolved catecholamine spikes correspond to single vesicle release from individual chromaffin cells. *Proc. Natl. Acad. Sc. USA* **88**, 10754-10758. (doi: N/A)

[27] For a review see: Amatore C, Arbault S, Guille M, Lemaître F. 2008 Electrochemical monitoring of single cell secretion: vesicular exocytosis and oxidative stress. *Chem. Rev.* **108**, 2585-2621. (doi: 10.1021/cr068062g)

[28] Kozminski KD, Gutman DA, Davila V, Sulzer D, Ewing AG. 1998 Voltammetric and pharmacological characterization of dopamine release from single exocytotic events at rat pheochromocytoma (PC12) cells *Anal. Chem*. **70**, 3123-3130. (doi: 10.1021/ac980129f)

[29] Schroeder TJ, Jankowski JA, Kawagoe KT, Wightman RM, Lefrou C, Amatore C. 1992 Analysis of diffusional broadening of vesicular packets of catecholamines released from biological cells during exocytosis. *Anal. Chem.* **64**, 3077-3083. (doi: 10.1021/ac00048a003)

[30] Ren L, Mellander L, Keighron J, Cans AS, Kurczy M, Svir I, Oleinick A, Amatore C, Ewing AG. 2016 The evidence for open and closed exocytosis as the primary release mechanism. *Q. Rev. Biophys*. **49***,* e12. (doi: 10.1017/s0033583516000081)

[31] Omiatek DM, Dong Y, Heien ML, Ewing AG. 2010 Only a fraction of quantal content is released during exocytosis as revealed by electrochemical cytometry of secretory vesicles. *ACS Chem. Neurosci.* **1**, 234-245. (doi: 10.1021/cn900040e)

[32] Oleinick A, Hu R, Ren B, Tian ZQ, Svir I, Amatore C. 2016 Theoretical model of neurotransmitter release during in vivo vesicular exocytosis based on a grainy biphasic nano-structuration of chromogranins within dense core matrixes. *J. Electrochem. Soc*. **163**, H3014-H3024. (doi: 10.1149/2.0031604jes)

[33] Hu R, Ren B, Lin CJ, Oleinick A, Svir I, Tian ZQ, Amatore C. 2016 How 'full' is 'full fusion' during exocytosis from dense core vesicles? Effect of SDS on 'quantal' release and final fusion pore size. *J. Electrochem. Soc.* **163**, H853-H865. (doi: 10.1149/2.1071609jes)

[34] Taupin C, Dvolaitzky M, Sauterey C. 1975 Osmotic pressure-induced pores in phospholipid vesicles. *Biochemistry* **14**, 4771-4775. (doi: 10.1021/bi00692a032)

[35] Sandre O, Moreaux L, Brochard-Wyart F. 1999 Dynamics of transient pores in stretched vesicles. *Proc. Natl. Acad. Sci. USA* **96**, 10591-10596. (doi: 10.1073/pnas.96.19.10591)

[36] Amatore C, Bouret Y, Midrier L. 1999 Time-resolved dynamics of the vesicle membrane during individual exocytotic secretion events, as extracted from amperometric monitoring of adrenaline exocytosis from chromaffin cells. *Chem. Eur. J.* **5**, 2151-2162. (doi: 10.1002/(SICI)1521-3765(19990702)5:7<2151::AID-CHEM2151>3.0.CO;2-R)

[37] Breckenridge LJ, Almers W. 1987 Final steps in exocytosis observed in a cell with giant secretory granules. *Proc. Natl. Acad. Sci. USA* **84**, 1945-1949. (doi: N/A)

[38] Whitaker M, Zimmerberg J. 1987 Inhibition of secretory granule discharge during exocytosis in sea urchin eggs by polymer solutions. *J. Physiol. (London)* **389**, 527-539. (doi: 10.1113/jphysiol.1987.sp016670)

[39] Zimmerberg J, Curran M, Cohen FS, Brodwick M. 1987 Simultaneous electrical and optical measurements show that membrane fusion precedes secretory granule swelling during exocytosis of beige mouse mast cells. *Proc. Natl. Acad. Sci. USA* **84**, 1585-1589. (doi: N/A)

[40] Nanavati C, Fernandez J. 1993 The secretory granule matrix: a fast-acting smart polymer. *Science* **259**, 963–965. (doi: 10.1126/science.8438154)

[41] Couteaux R, Pecot-Dechavassine M. 1970 Vésicules synaptiques et poches au niveau des « zones actives » de la jonction neuromusculaire. *CR Acad. Sci. (Paris)* **271**, 2346-2349. (doi: N/A)

[42] Heuser J, Reese T. 1981 Structural changes after transmitter release at the frog neuromuscular junction. *J. Cell Biol.* **88**, 564-580. (doi: 10.1083/jcb.88.3.564)

[43] Betz WJ, Mao F, Smith CB. 1996 Imaging exocytosis and endocytosis. *Curr. Opin. Neurobiol*. **6**, 365-371. (doi: 10.1016/S0959-4388(96)80121-8)

[44] It must be noted that, due to the two methods spatial resolution, fusion pores must have expanded to a sufficiently large size to be observable by TIRFM or EM. Hence, fusion pores with radii much smaller than those of vesicles may then appear in TIRFM or EM as featuring vesicles in a pre-release docking stage [25] or as undergoing Kiss-and-Run. Hence, small fusion pores may be common but undetectable by these methods though giving rise to massive neurotransmitter release detectable by amperometry. In this respect, it is noted that coupled TIRFM-amperometry experiments evidenced poor time-correlations between events expected to be characterized simultaneously by the two methods; see, e.g., Meunier A, Jouannot O, Fulcrand R, Fanget I, Bretou M, Karatekin E, Arbault S, Guille M, Darchen F, Lemaître F, Amatore C. 2011 Coupling Amperometry and Total Internal Reflection Fluorescence Microscopy at ITO Surfaces for Monitoring Exocytosis of Single Vesicles. *Angew. Chem. Int. Ed.* **50**, 5081-5084. (doi: 10.1002/anie.201101148) Even so, conclusions based on amperometry, TIRFM and EM are not necessarily contradictory. Indeed, would a fusion pore closes or enlarges after neurotransmitter release ends cannot be inferred from most amperometric measurements whenever the current has reached the baseline level when this occurs.

[45] Chan SA, Doreian B, Smith C. 2010 Dynamin and Myosin Regulate Differential Exocytosis from Mouse Adrenal Chromaffin Cells. *Cell. Mol. Neurobiol.* **30**, 1351-1357. (doi: 10.1007/s10571-010-9591-z)

[46] Chan SA, Smith C. 2003 Low frequency stimulation of mouse adrenal slices reveals a clathrin-independent, protein kinase C-mediated endocytic mechanism. *J. Physiol.* **553**, 707–717. (doi: 10.1113/jphysiol.2003.053918)

[47] Chan SA, Smith C. 2001 Physiological stimuli evoke two forms of endocytosis in bovine chromaffin cells. *J. Physiol.* **537**, 871–885. (doi: 10.1111/j.1469-7793.2001.00871.x)

[48] Smith C, Neher E. 1997 Multiple forms of endocytosis in bovine adrenal chromaffin cells. *J. Cell. Biol*. **139**, 885–894. (doi: 10.1083/jcb.139.4.885)

[49] O'Connor DT, Burton D, Deftos LJ. 1983 Immunoreactive human chromogranin A in diverse polypeptide hormone producing human tumors and normal endocrine tissues. *J. Clin. Endocrinol. Metabol*. **57***,* 1084-1086. (doi: 10.1210/jcem-57-5-1084)

[50] Romanova EV, Aerts JT, Croushore CA, Sweedler JV. 2014 Small-volume analysis of cell–cell signaling molecules in the brain. *Neuropsychopharmacol.* **39**, 50–64. (doi: 10.1038/npp.2013.145)

[51] For a review see: Park JJ, Loh YP. 2008 Minireview: How peptide hormone vesicles are transported to the secretion site for exocytosis. *Mol. Endocrinol*. **22**, 2583–2595. (doi: 10.1210/me.2008-0209)

[52] Barg S, Olofsson CS, Schriever-Abeln J, Wendt A, Gebre-Medhin S, Renström E, Rorsman P. 2002 Delay between fusion pore opening and peptide release from large dense-core vesicles in neuroendocrine cells. *Neuron* **33**, 287-299. (doi: 10.1016/S0896-6273(02)00563-9)

[53] Transport inside a still compact matrix may not proceed through classical diffusion (i.e., in the Einstein-Schmoluchowski sense) even across tortuous pathways, but through site-

hopping between occupied and free sites. However, following the general usage in such case, we use the term “diffusion” since it has been established that such “site-hopping” processes give rise to the same microscopic and macroscopic laws as classical diffusion. See, e.g., references [54-63].

[54] Dahms HJ. 1968 Electronic conduction in aqueous solution. *J. Phys. Chem.* **72**, 362-364. (doi: 10.1021/j100847a073)

[55] Ruff I, Friedrich VJ. 1971 Transfer diffusion. I. Theoretical. *J. Phys. Chem.* **75**, 3297-3302. (doi: 10.1021/j100690a016)

[56] Ruff I, Friedrich VJ, Demeter K, Csillag K. 1971 Transfer diffusion. II. Kinetics of electron exchange reaction between ferrocene and ferricinium ion in alcohols. *J. Phys. Chem.* **75**, 3303-3309. (doi: 10.1021/j100690a017)

[57] Murray RW, Goodenough JB, Albery WJ. 1981 Modified electrodes: chemically modified electrodes for electrocatalysis [and discussion]. *Phil. Trans. R. Soc., London A.*, **302**, 253-265. (doi: 10.1098/rsta.1981.0165)

[58] Andrieux CP, Savéant JM. 1980 Electron transfer through redox polymer films. *J. Electroanal. Chem.* **111**, 377-381. (doi: 10.1016/S0022-0728(80)80058-1)

[59] Laviron E. 1980 A multilayer model for the study of space distributed redox modified electrodes: Part I. Description and discussion of the model. *J. Electroanal. Chem.* **112**, 1-9. (doi: 10.1016/S0022-0728(80)80002-7)

[60] Blauch DN, Savéant JM. 1992 Dynamics of electron hopping in assemblies of redox centers. Percolation and diffusion. *J. Am. Chem. Soc.* **114**, 3323-3332. (doi: 10.1021/ja00035a025)

[61] Blauch DN, Savéant JM. 1993 Effects of long-range electron transfer on charge transport in static assemblies of redox centers. *J. Phys. Chem.* **97**, 6444-6448. (doi: 10.1021/j100126a019)

[62] Amatore C, Bouret Y, Maisonhaute E, Goldsmith JI, Abruña HD. 2001 Ultrafast voltammetry of adsorbed redox active dendrimers with nanometric resolution: an electrochemical microtome. *ChemPhysChem* **2**, 130-134. (doi: 10.1002/1439-7641(20010216)2:2<130::AID-CPHC130>3.0.CO;2-K)

[63] Amatore C, Bouret Y, Maisonhaute E, Goldsmith JI, Abruña HD. 2001 Precise adjustment of nanometric-scale diffusion layers within a redox dendrimer molecule by ultrafast cyclic voltammetry: an electrochemical nanometric microtome. *Chem. Eur. J.* **7**, 2206-2226. (doi: 10.1002/1521-3765(20010518)7:10<2206::AID-CHEM2206>3.0.CO;2-Y)

[64] Amatore C, Oleinick AI, Svir I. 2010 Diffusion from within a spherical body with partially blocked surface: diffusion through a constant surface area. *ChemPhysChem* **11**, 149-158. (doi: 10.1002/cphc.200900646)

[65] Amatore C, Oleinick AI, Svir I. 2010 Reconstruction of aperture functions during full fusion in vesicular exocytosis of neurotransmitters. *ChemPhysChem* **11**, 159-174. (doi: 10.1002/cphc.200900647)

[66] Oleinick A, Lemaître F, Guille-Collignon M, Svir I, Amatore C. 2013 Vesicular release of neurotransmitters: converting amperometric measurements into size, dynamics and energetics of initial fusion pores. *Faraday Discuss.* **164**, 33-55. (doi: 10.1039/c3fd00028a)

[67] Mellander LJ, Trouillon R, Svensson MI, Ewing AG. 2012 Amperometric post spike feet reveal most exocytosis is via extended kiss-and-run fusion. *Sci. Rep.* **2**, 907. (doi: 10.1038/srep00907)

[68] Trouillon R, Ewing AG. 2013 Amperometric measurements at cells support a role for dynamin in the dilation of the fusion pore during exocytosis. *ChemPhysChem* **14**, 2295-2301. (doi: 10.1002/cphc.201300319)

[69] Trouillon R, Ewing AG. 2014 Actin controls the vesicular fraction of dopamine released during extended kiss and run exocytosis. *ACS Chem. Biol*. **9**, 812-820. (doi: 10.1021/cb400665f)

[70] Mellander LJ, Kurczy ME, Najafinobar N, Dunevall J, Ewing AG, Cans AS. 2014 Two modes of exocytosis in an artificial cell. *Sci. Rep.* **4**, 3847. (doi: 10.1038/srep03847)

[71] Amatore C, Arbault S, Bonifas I, Lemaître F, Verchier Y. 2007 Vesicular exocytosis under hypotonic conditions shows two distinct populations of dense core vesicles in bovine chromaffin cells. *ChemPhysChem* **8**, 578-585. (doi: 10.1002/cphc.200600607)

[72] Amatore C, Arbault S, Bouret Y, Guille M, Lemaître F, Verchier Y. 2006 Regulation of exocytosis in chromaffin cells by trans-insertion of lysophosphatidylcholine and arachidonic acid into the outer leaflet of the cell membrane. *ChemBioChem* **7**, 1998-2003. (doi: 10.1002/cbic.200600194)

[73] A first experimental report of the systematic occurrence of exponential tails for amperometric spikes was provided by: Brioso MA, Gomez JF, Machado JD, Borges R. 2004 *Cell Biology of the Chromaffin Cell* (Eds., R. Borges, L. Gandia). Instituto Teofilo Hernando, Madrid-La Laguna, 211–216. (doi: N/A; ISBN 84-688-7007-2)

[74] It is noted that this is also fully consistent with the long time limit of the empirical Eqn (5) reported in: Schroeder TJ, Borges R, Pihel K, Amatore C, Wightman RM. 1996 Temporally resolved, independent stages of individual exocytotic secretion events. *Biophys. J.* **70**, 1061-1068 (doi: 10.1016/S0006-3495(96)79652-2), that has been used in earliest semi-empirical quantitative analyses of amperometric spikes recorded during stimulated release in chromaffin cells.

[75] Amatore C, Bouret Y, Travis ER, Wightman RM. 2000 Adrenaline release by chromaffin cells: constrained swelling of the vesicle matrix leads to full fusion. *Angew. Chem. Int. Ed.* **39**, 1952-1955. (doi: 10.1002/1521-3773(20000602)39:11<1952::AID-ANIE1952>3.0.CO;2-3)

[76] Amatore C, Bouret Y, Travis ER, Wightman RM. 2000 Interplay between membrane dynamics, diffusion and swelling pressure governs individual vesicular exocytotic events during release of adrenaline by chromaffin cells. *Biochim.* **82**, 481-496. (doi: 10.1016/S0300-9084(00)00213-3)

[77] Fan TH, Fedorov AG. 2004 Transport model of chemical secretion process for tracking exocytotic event dynamics using electroanalysis. *Anal. Chem*. **76**, 4395-4405. (doi: 10.1021/ac049748g)

[78] Coupland RE. 1968 Determining sizes and distribution of sizes of spherical bodies such as chromaffin granules in tissue sections. *Nature* **217**, 384–388. (doi: 10.1038/217384a0)

[79] For determining κ in reference [66], we relied on (a) the mean current intensities of the pres-spike features, and (b) on the $R_{\mathrm{pore}}^{\mathrm{initial}}$= 1.2 nm value measured by patch-clamp for the radius of the initial fusion pore [20]. If the patch-clamp community reevaluates this value by a factor γ, all $R_{\mathrm{pore}}(t)$ values reported in this work need to be rescaled by the same factor γ since κ is, by construction of the extraction procedure [66], proportional to $1/R_{\mathrm{pore}}^{\mathrm{initial}}$ while $R_{\mathrm{pore}}(t)$ is proportional to $1/\kappa$, see Eqn (6). Hence, the absolute values reported here are ultimately proportional to the size adopted for $R_{\mathrm{pore}}^{\mathrm{initial}}$. Interestingly, using $R_{\mathrm{ves}} = 156\ \mathrm{nm}$ for the mean vesicle radius [78], $\kappa = 415\ \mathrm{s}^{-1}$ corresponds to $D_{\mathrm{ves}} = 10^{-7}\ \mathrm{cm}^2\ \mathrm{s}^{-1}$, i.e., to a value ca 50 times less than in aqueous media, a fact that seems consistent with a polyelectrolyte gel. Note that, for each individual event, κ is susceptible to variations with an exponential distribution [66]. This is the reason for which we relied on the statistical analyses of hundreds of spikes, for which these random variations should compensate. In other words, the $R_{\mathrm{pore}}(t)$ values reported in Figures 1Aa-e should better viewed as illustrative since each may suffer a small random scaling factor. Conversely, the data reported in Figures 1Ba-e and 1Ca-e should be immune to such random effects through statistical auto-compensation.

[80] Israelachvili JN, Mitchell DJ, Ninham BW. 1976 Theory of self-assembly of hydrocarbon amphiphiles into micelles and bilayers. *J. Chem. Soc. Faraday Trans*. *2* **72**, 1525-1568. (doi: 10.1039/F29767201525)

[81] Allende D, Simon SA, McIntosh TJ. 2005 Melittin-induced bilayer leakage depends on lipid material properties: evidence for toroidal pores. *Biophys. J*. **88**, 1828-1837. (doi: 10.1529/biophysj.104.049817)

[82] Morris DAN, McNeil R, Castellino FJ, Thomas JK. 1980 Interaction of lysophosphatidylcholine with phosphatidylcholine bilayers. A photo-physical and NMR study. *Biochim. Biophys. Acta, Biomembr*. **599**, 380-390. (doi: 10.1016/0005-2736(80)90185-6)

[83] Fuller N, Rand RP. 2001 The influence of lysolipids on the spontaneous curvature and bending elasticity of phospholipid membranes. *Biophys. J*. **81**, 243-254. (doi: 10.1016/S0006-3495(01)75695-0)

[84] Grote E, Baba M, Ohsumi Y, Novick PJ. 2000 Geranylgeranylated SNAREs are dominant inhibitors of membrane fusion. *J. Cell Biol*. **151**, 453-466. (doi: 10.1083/jcb.151.2.453)

[85] Chernomordik L, Chanturiya A, Green J, Zimmerberg J. 1995 The hemifusion intermediate and its conversion to complete fusion: regulation by membrane composition. *Biophys. J*. **69**, 922-929. (doi: 10.1016/S0006-3495(95)79966-0)

[86] Julicher F, Lipowsky R. 1996 Shape transformations of vesicles with intramembrane domains. *Phys. Rev. E*. **53**, 2670-2683. (doi: 10.1103/PhysRevE.53.2670)

[87] Cans AS, Wittenberg N, Karlsson R, Sombers L, Karlsson M, Orwar O, Ewing A. 2003 Artificial cells: Unique insights into exocytosis using liposomes and lipid nanotubes. *Proc. Natl. Acad. Sci. USA* **100**, 400-404. (doi: 10.1073/pnas.232702599)

[88] Harata NC, Aravanis AM, Tsien RW. 2006 Kiss-and-run and full-collapse fusion as modes of exo-endocytosis in neurosecretion. *J. Neurochem*. **97**, 1546–1570. (doi: 10.1111/j.1471-4159.2006.03987.x)

[89] Ryan TA. 2003 Kiss-and-run, fuse-pinch-and-linger, fuse-and-collapse: The life and times of a neurosecretory granule. *Proc. Natl. Acad. Sci. USA* **100**, 2171-2173. (doi: 10.1073/pnas.0530260100)

[90] Kusumi A, Umemura Y, Morone N, Fujiwara T. 2008 Chapter 19. Paradigm Shift of the Molecular Dynamics Concept in the Cell Membrane: High-Speed Single-Molecule Tracking Revealed the Partitioning of the Cell Membrane. *Anomalous Transport: Foundations and Applications* (Klages R, Radons R, Sokolov IM Eds), Wiley, New York. (doi: 10.1002/9783527622979.ch19)

[91] Kusumi A, Nakada C, Ritchie K, Murase K, Suzuki K, Murakoshi H, Kasai RS, Kondo J, Fujiwara T. 2005 Paradigm shift of the plasma membrane concept from the two-dimensional continuum fluid to the partitioned fluid: high-speed single-molecule tracking of membrane molecules. *Annu. Rev. Biophys. Biomol. Struct.* **34**, 351-378. (doi: 10.1146/annurev.biophys.34.040204.144637)

[92] Kusumi A, Sako Y. 1996 Cell surface organization by the membrane skeleton. *Curr. Opinion Cell Biol.* **8**, 566-574. (doi: 10.1016/S0955-0674(96)80036-6)

[93] Murakoshi H, Iino R, Kobayashi T, Fujiwara T, Ohshima C, Yoshimura A, Kusumi A. 2004 Single-molecule imaging analysis of Ras activation in living cells. *Proc. Natl. Acad. Sci. U.S.A.* **101**, 7317-7322. (doi: 10.1073/pnas.0401354101)

[94] In all cases, $v_{\mathrm{open}}^{\mathrm{max}}$ values resulted compatible with those recorded for pores dynamics in tensed GUV bilayers membranes [36]. It is also noted that $v_{\mathrm{open}}^{\mathrm{max}}$ values resulted considerably smaller than the sound velocity in bilipidic membranes (see, e.g., Griesbauer J, Wixforth A, Schneider MF. 2009 Wave propagation in lipid monolayers. *Biophys J*. **97**, 2710-2716. (doi: 10.1016/j.bpj.2009.07.049)) confirming that the expansion rates are regulated by viscous dissipation of membrane tension energies [36,77].

[95] Gillespie DT. 1977 Exact stochastic simulation of coupled chemical reactions. *J. Phys. Chem*. **81**, 2340-2361. (doi: 10.1021/j100540a008)

[96] For a recent discussion see: Singh PS, Lemay SG. 2016 Stochastic processes in electrochemistry. *Anal.Chem*. **88**, 5017-5027. (doi: 10.1021/acs.analchem.6b00683)

Table 1. Median and quartile values of fusion pores maximal sizes, $R_{\mathrm{pore}}^{\mathrm{max}}$, and maximal opening rates, $v_{\mathrm{open}}^{\mathrm{max}}$, as deduced from the probability densities shown in Figures 1B and 1C under different release conditions.[a]

Conditions[c]	$R_{\mathrm{pore}}^{\mathrm{max}}$ / nm[b]	$v_{\mathrm{open}}^{\mathrm{max}}$ / µm.s-1 [b]
Controls	16.8 (12.6; 20.2)	1.41 (0.74; 2.41)
Hypertonic	10.6 (6.6; 15.9)	0.74 (0.35; 1.84)
Hypotonic	20.3 (16.8; 21.9)	1.42 (0.93; 2.21)
AA-modified	11.4 (8.2; 15.3)	0.66 (0.40; 1.14)
LPC-modified	17.0 (15.0; 20.1)	1.65 (1.32; 2.42)

[a] Vesicular release elicited from chromaffin cells by 2mM Ba^{2+} (in Locke buffer supplemented with 0.7 mM $MgCl_2$, without carbonates) injection during 2s. [b] Median values (first and third quartile values reported between parentheses) based on Eqn (6) with $R_{\mathrm{ves}} = 156\ \mathrm{nm}$ [78], and $\kappa = D_{\mathrm{ves}}/R_{\mathrm{ves}}^2 = 415\ \mathrm{s}^{-1}$ [64-66] (see text). [c] Amperometric spikes measured at bovine chromaffin cells with 7 µm diameter carbon fiber microelectrodes held at 0.65 V vs. Ag/AgCl, see Section SM3 in SM and references [71, 72] for experimental details

Figure 1

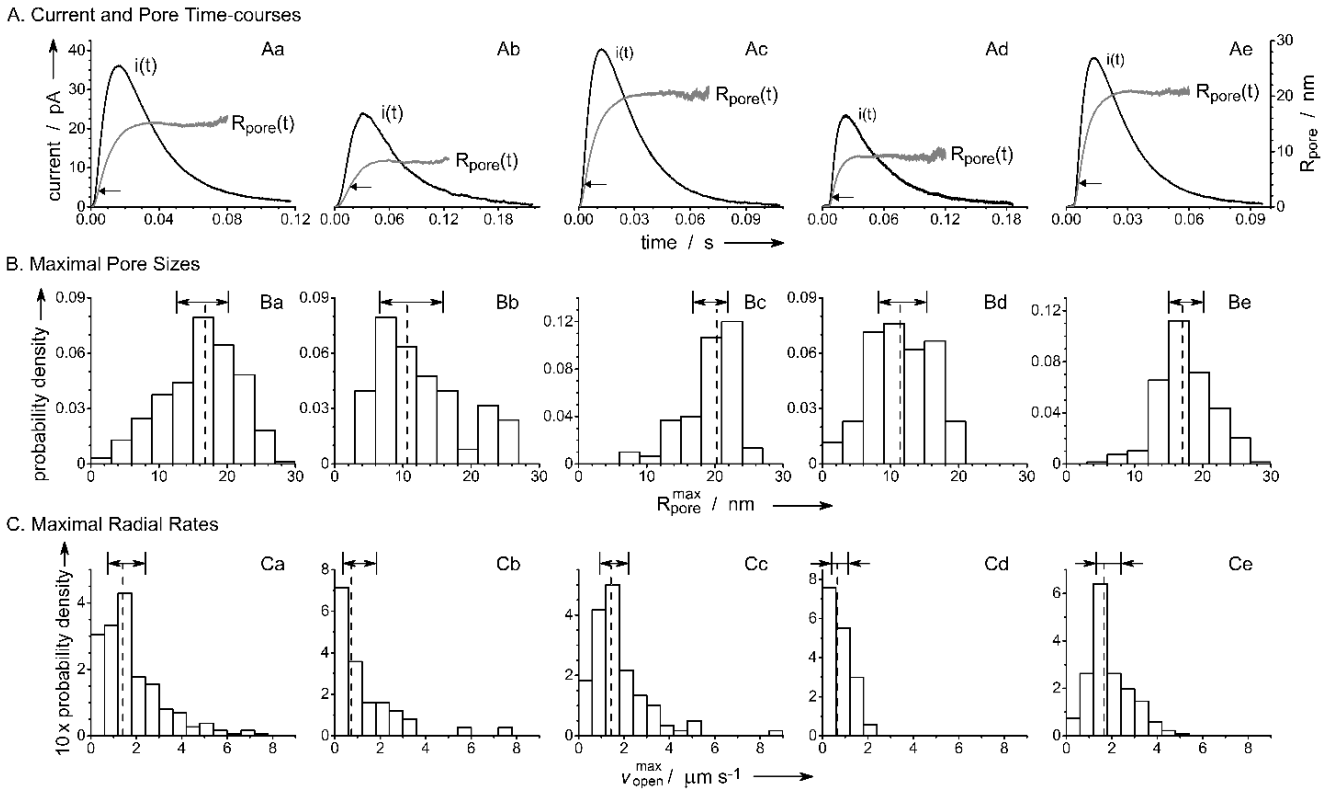

Figure 1. (A) Representative time-variations of the fusion pore radius, R_{pore}, superimposed onto the corresponding amperometric spikes recorded under several conditions [71, 72]: (a) controls; (b) hyper- or (c) hypotonic shock; (d) AA- or (e) LPC-modified cell membrane; the same code applies to the sequence of panels (a-e) in (B) and (C). (B) Statistical distributions of the maximal pore radii, $R_{\mathrm{pore}}^{\mathrm{max}}$, and (C) of the maximal radial expansion rates, $v_{\mathrm{open}}^{\mathrm{max}}$, as a function of the condition. The horizontal arrows in (A) indicate the R_{pore} values at which $v_{\mathrm{open}}^{\mathrm{max}}$ was achieved. In (B) and (C) the vertical dashed lines indicate the median values while the double-arrowed segments feature the first and third quartiles ones (see Table 1 for the corresponding numerical values).